hep-ph/9606214
DPNU-96-21

The Influence of the Full Vertex and Vacuum Polarization on the Fermion Propagator in QED3

P. Maris*
Department of Physics, Nagoya University, Nagoya 464-01, Japan
(April 1996)

Abstract

We investigate the influence of the full vacuum polarization and vertex function on the fermion propagator, using the coupled Dyson–Schwinger equations for the photon and fermion propagator. We show that, within a range of vertex functions, the general behavior of the fermion propagator does not depend on the exact details of the vertex, both in the massless and in the massive phase. Independent of the precise vertex function, there is a critical number of fermion flavors for dynamical mass generation in $(2+1)$-dimensional QED. A consistent treatment of the vacuum polarization is essential for these results.

11.10.Kk,11.15.Tk,11.30.Qc,11.30.Rd

I. INTRODUCTION

Quantum electrodynamics in 2 space- and 1 time-dimension, QED3, has several interesting features. It exhibits dynamical mass generation [1–10] and confinement [11–13], similar to QCD. Furthermore, it is superrenormalizable, so it does not suffer from the ultraviolet divergences which are present in QED4. The coupling constant is dimensionful, and provides us with a mass scale, even if we consider massless fermions. This energy scale plays the role of the QCD scale Λ_{QCD}, in the sense that it sets the scale for confinement and dynamical mass generation. Thus it is a very interesting model to study these nonperturbative phenomena.

QED3 also has some applications in condensed matter physics, where it can be regarded as an effective theory for more realistic microscopic models [14,15]. Especially, since the discovery of high-T_c superconductivity and the fractional quantum Hall effect, these kinds of models have attracted more attention.

In this paper, we consider QED3 with N fermion flavors of four-component spinors. Such a model of QED3 is chirally symmetric in the absence of a bare fermion mass term, $m_0\bar{\psi}\psi$, in contrast to the (2+1)-dimensional gauge theory with two-component fermions, where we cannot define chiral symmetry [1,2,16]. Similar to the four-dimensional case [17], the chiral symmetry of QED3 may be broken spontaneously due to the dynamical generation of a fermion mass. The question of whether or not chiral symmetry is broken for all values of N, the number of fermion flavors, is very interesting.

We address this question by analyzing the behavior of the full fermion propagator nonperturbatively, using its Dyson–Schwinger equation. However, this equation cannot be solved without truncating the infinite set of Dyson–Schwinger equations, since it involves the full photon propagator and the full vertex function. Different ways of truncating this equation give rise to different results concerning the question of whether there is a critical number of fermion flavors for dynamical mass generation [2,3,6–9]. In this paper we try to resolve the controversy.

Using the bare vertex approximation and the one-loop vacuum polarization, Appelquist *et al.* [2] have shown that there is a finite critical number of flavors N_c, above which the chiral symmetry is restored. They found in Landau gauge a critical value of $N_c = 32/\pi^2 \simeq 3.24$. This approach is based on a $1/N$ expansion, and including the next-to-leading-order terms [3], it was found that the critical number changes to $N_c = 128/3\pi^2 \simeq 4.32$.

However, such a simple treatment was criticized by Pennington *et al.* [6], since the effects of the wavefunction renormalization were not taken into account. The problem is that formally the wavefunction renormalization is of order $1 + \mathcal{O}(1/N)$, but in the infrared region, this wavefunction renormalization tends to vanish. Because of this non-uniformity in the $1/N$ expansion, an approximation based on an expansion in $1/N$ might not be very reliable. Taking into account wavefunction renormalization, Pennington *et al.* found chiral symmetry breaking for all numbers of fermion flavors. However, as we show, their approach also has some inconsistency.

There have been several attempts to resolve the problem, by means of more sophisticated Ansätze for the full vertex [7–10], and by use of a so-called nonlocal gauge-function [18–20], but none of them are completely satisfactorily. Also other methods, such as the inversion method [21], ϵ-expansion [22], and lattice calculations [5], have not given a final answer to

this question, although the lattice results favor the existence of a finite critical number of fermion flavors [5,23]. The difficulty is that it is numerically very difficult to observe the exponential decrease of the dynamical mass for increasing N found in [6,7].

In our paper, the existence of a finite critical number of flavors is confirmed by analyzing the *coupled* Dyson–Schwinger equations, for both the fermion and the photon propagator, using several different approximations for the full vertex. We show that, within a certain class of vertex Ansätze, there is a critical number of fermion flavors for dynamical mass generation in QED3. This number does not depend very strongly on the precise form of the vertex Ansatz. Also the general behavior of the fermion propagator does not depend on the exact details of the Ansatz. The essential point is to take into account the full vacuum polarization in a consistent way.

In the next section, we describe the formalism in more detail, together with our truncation scheme. Before addressing the question of chiral symmetry breaking, we first analyze the full fermion propagator in the massless phase, see Sec. III. This already yields some nontrivial results, namely that the structure of the massless full fermion propagator is almost independent of our Ansatz. In Sec. IV, we discuss dynamical mass generation, and show that there is a critical number of fermion flavors for chiral symmetry breaking, $N_c \simeq 3.3$, almost independent of our choice for the vertex. Finally we give some concluding remarks in Sec. V.

II. FORMALISM

A. Three-dimensional QED with N massless fermion flavors

We consider QED3 with N massless fermion flavors, and choose to work in Euclidean space, ignoring the issues discussed in [13]. The Lagrangian in a general covariant gauge is given by

$$\mathcal{L} = \sum_{i=0}^{N} \bar{\psi}_i (i \not{\partial} + e \not{A}) \psi_i + \tfrac{1}{4} F_{\mu\nu}^2 + \tfrac{1}{2a} (\partial_\mu A_\mu)^2 \,. \tag{1}$$

We use four-component spinors for the fermions, and accordingly a four-dimensional representation for the γ-matrices. With such a representation we can define chirality just as in four-dimensional QED. This chiral symmetry can be broken dynamically by generation of a mass for the fermions. In this formulation, there can also be a parity breaking mass term, which conserves the chiral symmetry, but it is known that such a mass is not generated dynamically [16].

We have N fermion flavors, and consider both the large N limit, as well as the quenched limit, $N \downarrow 0$. In the quenched limit, the mass scale is defined by the dimensionful coupling constant e^2, and there are no free parameters. Outside the quenched limit, N, the number of fermion flavors is the only free parameter. When using the large N expansion [2], we keep the product Ne^2 finite, and it is most convenient to define the mass scale by

$$\alpha = \frac{Ne^2}{8} \,. \tag{2}$$

B. Dyson–Schwinger equations for the propagators

The Dyson–Schwinger (DS) equation for the fermion propagator is given by

$$S^{-1}(p) = S_0^{-1}(p) - e^2 \int \frac{\mathrm{d}^3k}{(2\pi)^3} \gamma_\mu S(k) \Gamma_\nu(p,k) D_{\mu\nu}(p-k)\,. \tag{3}$$

Since parity is not broken dynamically, we can decompose the fermion propagator into

$$S^{-1}(p) = A(p)\, \not{p} + B(p)\,, \tag{4}$$

and rewrite the DS equation into

$$A(p) = 1 + \frac{e^2}{p^2} \int \frac{\mathrm{d}^3k}{(2\pi)^3} \tfrac{1}{4} \mathrm{Tr}[\, \not{p}\, \gamma_\mu S(k) \Gamma_\nu(p,k) D_{\mu\nu}(p-k)]\,, \tag{5}$$

$$B(p) = e^2 \int \frac{\mathrm{d}^3k}{(2\pi)^3} \tfrac{1}{4} \mathrm{Tr}[\gamma_\mu S(k) \Gamma_\nu(k,p) D_{\mu\nu}(p-k)]\,. \tag{6}$$

The problem in analyzing this equation is the full vertex and full photon propagator. For the photon propagator we also have a DS equation, namely

$$D_{\mu\nu}^{-1}(q) = {D_0^{-1}}_{\mu\nu}(q) - e^2 \int \frac{\mathrm{d}^3k}{(2\pi)^3} \gamma_\mu S(k) \Gamma_\nu(k, p-k) S(p-k)\,, \tag{7}$$

without introducing new unknown functions. It is more convenient to write this last expression in terms of the vacuum polarization tensor $\Pi_{\mu\nu}(q)$

$$\Pi_{\mu\nu}(q) = e^2 \int \frac{\mathrm{d}^3k}{(2\pi)^3} \gamma_\mu S(k) \Gamma_\nu(k, p-k) S(p-k)\,. \tag{8}$$

Since the longitudinal part of the photon propagator is not affected by the interactions, because of gauge invariance, we can write the full photon propagator in a general covariant gauge

$$D_{\mu\nu}(q) = -\left(\delta_{\mu\nu} - \frac{q_\mu q_\nu}{q^2}\right) \frac{1}{q^2 + \Pi(q)} - a \frac{q_\mu q_\nu}{q^4}\,, \tag{9}$$

with the vacuum polarization $\Pi(q)$ defined by

$$\Pi_{\mu\nu}(q) = \left(\delta_{\mu\nu} - \frac{q_\mu q_\nu}{q^2}\right) \Pi(q)\,. \tag{10}$$

The vacuum polarization tensor has an ultraviolet divergence, which can be removed by a gauge-invariant regularization scheme. However, this divergence is only present in the longitudinal part, so by contracting $\Pi_{\mu\nu}(q)$ with

$$q^2 \delta_{\mu\nu} - 3 \frac{q_\mu q_\nu}{q^2}\,, \tag{11}$$

we can project out the finite vacuum polarization $\Pi(q)$ [11]. So, the coupled DS equations for the photon and fermion propagator form a set of three coupled equations for three scalar functions, and the only unknown function is the full vertex function. Note that both the DS equation for the fermion propagator, and the one for the photon propagator, are exact.

In principle, we could write down a DS equation for the full vertex function as well, but this will not lead to a closed set of equations: the DS equation for the vertex involves a four-point function, and so on. The full set of DS equations forms an infinite hierarchy of coupled integral equations for the Green's functions. In order to solve the DS equation for a particular Green's function, we have to truncate or approximate this infinite set of equations. For calculating the propagators, we must find a reasonable approximation for the full vertex function $\Gamma^\mu(p,k)$.

C. Truncation scheme

Now, what is a reasonable approximation for the full vertex function? The most simple and in some sense "natural" approximation is to take the leading order perturbative vertex

$$\Gamma_\mu \to \gamma_\mu \,. \tag{12}$$

This truncation is commonly used in studies of the fermion DS equation, and it is usually referred to as ladder or rainbow approximation, since it generates rainbow diagrams in the fermion DS equation, and ladder diagrams in the Bethe-Salpeter equation for the fermion–anti-fermion bound state amplitude. In principle there is a systematic way to improve this truncation, namely by taking the next-to-leading order vertex function, and so on.

The obvious disadvantage of this approach is that it relies on perturbation theory, whereas the DS equations are nonperturbative equations. Until one performs the complete next-to-leading order calculation, one does not know how reliable the leading order calculation is. Even after obtaining such a next-to-leading order, there remains some doubt about the validity of this approach, due to the non-uniformity of the $1/N$ expansion.

Furthermore, as a consequence on the one hand of using a nonperturbative method to calculate some Green's functions, and on the other hand of employing perturbation theory for other Green's functions, one violates the Ward–Takahashi (WT) identities relating these Green's functions, and loses gauge covariance. To be specific, the WT identity relating the full vertex to the fermion propagator

$$q_\mu \Gamma_\mu = S^{-1}(p) - S^{-1}(k)\,, \tag{13}$$

is an exact identity, which holds order-by-order in perturbation theory, but if one uses perturbation theory to approximate the full vertex, and the truncated DS equation to calculate the fermion propagator, one will (in general) violate this identity.

Instead of using a perturbative approximation for the vertex function, one can also use other nonperturbative information to make an Ansatz for the full vertex. The full vertex can be decomposed into 12 different Lorentz structures, and four of them are uniquely determined by the WT identity [24]. So by imposing the WT identity, we can write the full vertex as

$$\Gamma_\mu = \tfrac{1}{2}(A(p)+A(k))\gamma_\mu + \tfrac{1}{2}(\not{p}+\not{k})(p_\mu+k_\mu)\frac{A(p)-A(k)}{p^2-k^2}$$
$$-(p_\mu+k_\mu)\frac{B(p)-B(k)}{p^2-k^2}+\dots\,, \tag{14}$$

where the dots represent the part of the vertex not constrained by the WT identity. Now one can simply neglect that unconstrained part, and take the above expression as Ansatz (usually called Ball–Chiu vertex) for the full vertex. However, a perturbative calculation shows that the unconstrained part is not zero [25], and by just neglecting it you never see what you are throwing away.

The WT identity is not the only requirement one can impose on the full vertex function. Other requirements are that it reduces to the bare vertex in the weak coupling limit, and multiplicative renormalizability also restricts the full vertex, even in a superrenormalizable theory like QED3. Furthermore, any Ansatz should have the correct symmetry properties. However, all these constraints do not uniquely determine the full vertex, they all leave parts of the vertex undetermined. So the results might depend heavily on the particular choice for the vertex. Another disadvantage of using a vertex Ansatz is that it is not possible to improve the approximation in a systematic way.

D. Vertex Ansätze

In this paper, we use several different Ansätze for the full vertex, including a bare vertex, and compare the results to see how much influence these different choices have on the propagators. For the sake of simplicity, we consider the form

$$\Gamma_\mu(p,k) = f(A(p),A(k),A(p-k))\gamma_\mu\,, \tag{15}$$

with the restriction that for $A(p)\equiv 1$, the full vertex reduces to the bare vertex. This automatically ensures that in the weak coupling limit, the full vertex reduces to the bare one. Such an Ansatz has the same tensor structure as the bare vertex, and by restricting ourselves to this tensor structure, we simplify the numerical integrations considerably. It is also generally expected that this tensor structure plays the most dominant role in the full vertex.

To be more specific, we will analyze the coupled DS equations for the propagators, using the following choices for $f(A(p),A(k),A(p-k))$:

1. the bare vertex: $f(A(p),A(k),A(q))=1$
2. a simple Ansatz inspired by the Ball–Chiu vertex Eq. (14) [24]: $f=\frac{1}{2}(A(p)+A(k))$
3. $f=A(p)A(k)/A(q)$
4. $f=\frac{1}{4}(A(p)+A(k))^2$
5. $f=A(p)A(k)$.

Of these choices, only the first two are actually motivated on physical arguments. The last one is primarily motivated by the fact that the resulting truncated DS equations are easy to solve analytically (at least in the symmetric phase). The choices 3 and 4 are merely added in order to see how much the results depend on our particular choice; Ansatz 3 is based on 5, but linear in the wavefunction renormalization, as it is supposed to be, whereas Ansatz 4 is the quadratic form of Ansatz 2. The last two Ansätze are also inspired by the suggestion in [8] that the effective vertex correction in the fermion DS equation is quadratic in the wavefunction renormalization.

Finally, we have to choose a gauge, and since the Landau gauge is the most convenient and commonly used gauge, we use it. Using the Ansatz for the vertex we have just described, the DS equations for the propagators reduce to

$$A(p) = 1 + \frac{2\,e^2}{p^2}\int\frac{\mathrm{d}^3k}{(2\pi)^3}\frac{A(k)(p\cdot q)(k\cdot q)}{A^2(k)k^2+B(k)}\frac{f(A(p),A(k),A(q))}{q^2(q^2+\Pi(q))}\,, \tag{16}$$

$$B(p) = 2\,e^2\int\frac{\mathrm{d}^3k}{(2\pi)^3}\frac{B(k)}{A^2(k)k^2+B(k)}\frac{f(A(p),A(k),A(q))}{q^2+\Pi(q)}\,, \tag{17}$$

$$\Pi(q) = Ne^2\int\frac{\mathrm{d}^3k}{(2\pi)^3}\left(2k^2-4k\cdot q-\frac{6k\cdot q}{q^2}\right)\frac{A(k)}{A^2(k)k^2+B^2(k)}\,\frac{A(p)f(A(p),A(k),A(q))}{A^2(p)p^2+B^2(p)}, \tag{18}$$

with $q = p - k$.

III. SYMMETRIC PHASE

First, we consider the massless fermion phase, so $B(p) \equiv 0$, which is always a solution of Eq. (17). This reduces the problem to solving two coupled equations, one for the wavefunction renormalization $A(p)$, and one for the vacuum polarization $\Pi(p)$.

A. Analytical results

With $B(p) \equiv 0$, the vacuum polarization reduces to

$$\Pi(q) = Ne^2\int\frac{\mathrm{d}^3k}{(2\pi)^3}\frac{2k^2-4k\cdot q-6(k\cdot q)/q^2}{k^2(k+q)^2}\frac{f(A(k+q),A(k),A(q))}{A(k)A(k+q)}\,. \tag{19}$$

We first consider Ansätze 3 and 5, because the vacuum polarization can then be calculated analytically. With Ansatz 3, the vacuum polarization becomes

$$\Pi(q) = Ne^2q/(8A(q)) = \alpha q/A(q)\,, \tag{20}$$

whereas Ansatz 5 leads to

$$\Pi(q) = Ne^2q/8 = \alpha q\,. \tag{21}$$

In the massless phase, the equation for the wavefunction renormalization becomes

$$A(p) = 1 + \frac{2\,e^2}{p^2}\int\frac{\mathrm{d}^3k}{(2\pi)^3}\frac{f(A(p),A(k),A(q))}{A(k)k^2}\frac{(p\cdot q)(k\cdot q)}{q^2(q^2+\Pi(q))}\,. \tag{22}$$

For the Ansätze 3 and 5, this can now be reduced to

$$A(p) = 1 + A(p)\frac{16\alpha}{Np^2}\int \frac{\mathrm{d}^3k}{(2\pi)^3}\frac{1}{A(q)q^2+\alpha q}\frac{(p\cdot q)(k\cdot q)}{k^2q^2}\,, \tag{23}$$

$$A(p) = 1 + A(p)\frac{16\alpha}{Np^2}\int \frac{\mathrm{d}^3k}{(2\pi)^3}\frac{1}{q^2+\alpha q}\frac{(p\cdot q)(k\cdot q)}{k^2q^2}\,, \tag{24}$$

where we use $\alpha = N\,e^2/8$ rather than e^2 to define the energy scale. This last equation can be solved exactly

$$A^{-1}(p) = 1 - \frac{2\alpha}{Np^2\pi^2}\int_0^\infty \frac{\mathrm{d}q}{q^2+\alpha q}\left(q^2 - p^2 - \frac{q^4-p^4}{2pq}\ln\frac{p+q}{|p-q|}\right)\,, \tag{25}$$

whereas Eq. (23) gives a nonlinear integral equation for $A(p)$

$$A^{-1}(p) = 1 - \frac{2\alpha}{Np^2\pi^2}\int_0^\infty \frac{\mathrm{d}q}{A(q)q^2+\alpha q}\left(q^2 - p^2 - \frac{q^4-p^4}{2pq}\ln\frac{p+q}{|p-q|}\right)\,, \tag{26}$$

and thus gives an implicit relation for the wavefunction renormalization.

However, both Ansätze lead to the same explicit expression, if we make one further approximation, which is commonly used in this context. In the infrared region, $q \ll \alpha$, the vacuum polarization dominates: the denominators, $A(q)q^2 + \alpha q$ in Eq. (23), and $q^2 + \alpha q$ in Eq. (24), both behave like αq, whereas for large momenta, $q \gg \alpha$, the wavefunction renormalization is almost equal to one, and the contribution to these denominators coming from the vacuum polarization can be neglected. So in both cases the wavefunction renormalization behaves like

$$\begin{aligned} A^{-1}(p) &\simeq 1 - \frac{2\alpha}{Np^2\pi^2}\left(\int_0^\alpha \frac{\mathrm{d}q}{\alpha q} + \int_\alpha^\infty \frac{\mathrm{d}q}{q^2}\right)\left(q^2 - p^2 - \frac{q^4-p^4}{2pq}\ln\frac{p+q}{|p-q|}\right) \\ &= 1 - \frac{1}{N\pi^2}\left(1 - \frac{\alpha^2}{3p^2} - \frac{3p^4+6p^2\alpha^2-\alpha^4}{6p^3\alpha}\ln\frac{\alpha+p}{|\alpha-p|} - \frac{4}{3}\ln\frac{|\alpha^2-p^2|}{p^2}\right)\,. \end{aligned} \tag{27}$$

B. Numerical results

We can also solve the integral equations for the wavefunction renormalization and the vacuum polarization numerically. Starting with bare propagators to calculate the vacuum polarization, we solve Eq. (16) with this vacuum polarization. Using this solution for the wavefunction renormalization, we again calculate the vacuum polarization and repeat this procedure until the solutions for both $\Pi(p)$ and $A(p)$ converge to a stable solution. In Fig. 1, we have plotted the analytic solutions for the wavefunction renormalization as described in the previous section, together with our numerical result. We see that they agree very well with each other qualitatively, and that in the ultraviolet region the $A(p)$ is almost equal to one, as expected, whereas in the infrared region, it deviates considerably from the perturbative value. In particular, it is important to notice that for $p \downarrow 0$, the wavefunction renormalization vanishes, as also can be seen from Eq. (27).

For the other vertex Ansätze, we cannot solve the integral equations analytically. Numerically, we find a very similar behavior for the wavefunction renormalization for all five different Ansätze, as is shown in Fig. 2(a). The vacuum polarization also seems to be quite insensitive to the vertex Ansatz, as can be seen from Fig. 2(b). So it turns out that the exact form of the Ansatz is not very relevant for the behavior of the fermion propagator, *provided that one uses a consistent approximation scheme*: consider the coupled equations for the fermion and photon propagators, and use the same approximation for the full vertex in both the fermion and the photon DS equation. However, the *deviation* of the vacuum polarization from the perturbative leading-order behavior

$$\Pi(q) = \alpha q \,, \tag{28}$$

does depend strongly on the Ansatz, see Fig. 2(c).

It can be explained that the different vertex Ansätze lead to the same behavior for the wavefunction renormalization. In the symmetric phase, Eqs. (16)–(18) reduce to

$$A(p) = 1 + \frac{2\,e^2}{p^2} \int \frac{\mathrm{d}^3k}{(2\pi)^3} \frac{f(A(p), A(k), A(q))}{A(k)k^2} \frac{(p\cdot q)(k\cdot q)}{q^2(q^2+\Pi(q))} \,, \tag{29}$$

$$\Pi(q) = Ne^2 \int \frac{\mathrm{d}^3k}{(2\pi)^3} \frac{(2k^2 - 4k\cdot q - 6(k\cdot q)/q^2) f(A(p), A(k), A(q))}{A(k)A(p)\,k^2p^2} \,. \tag{30}$$

In the ultraviolet region, the propagators, and also the full vertices, reduce to the bare ones, so the crucial region is the infrared region. In the (far) infrared region, the vacuum polarization dominates in the denominator of the kernel of Eq. (29), $q^2 + \Pi(q)$, so we can approximate this denominator by $\Pi(q)$. We can now observe that there is a cancellation in the infrared region between the different effects of the vertex Ansatz: the function f enters the integral equation both in the numerator, and, via the vacuum polarization, in the denominator. The remaining equation for the wavefunction renormalization resembles the Eqs. (23) and (24), which we have analyzed in the previous subsection. This cancellation explains why we get a very similar behavior for the wavefunction renormalization, using quite different Ansätze for the vertex.

Note that for such a cancellation, the vacuum polarization has to depend quite strongly on the precise Ansatz, and in Fig. 2(c) we see that the deviation from the perturbative behavior is indeed governed by the powers of $A(p)$ in our vertex Ansatz. Using a bare vertex, the vacuum polarization becomes quadratic in $1/A$, with a vertex linear in A, the vacuum polarization becomes linear in $1/A$ and with an Ansatz which is quadratic in the wavefunction renormalization, the vacuum polarization does not contain any powers of A, and is (almost) equal to the perturbative one.

Finally, we show in Fig. 3 the wavefunction renormalization for several different numbers of fermion flavors. This shows that there is only a quantitative dependence on the number of flavors, as long as we stay in the symmetric phase. The other Ansätze yield a similar result.

C. Infrared Behavior

As can be seen from Eq. (27), the wavefunction renormalization vanishes in the infrared region, in contrast to what one might expect based on ordinary perturbation theory or the

$1/N$ expansion. Such a vanishing behavior could very well be related to an anomalous dimension for the wavefunction renormalization as suggested in [8,26]. It has been argued that the naive perturbative behavior

$$A_{\rm pert}(p) \simeq 1 + \frac{8}{3N\pi^2} \ln\left(p/\alpha\right), \tag{31}$$

is the first term of the build-up of an anomalous dimension

$$A(p) \simeq \left(\frac{p}{\alpha}\right)^{\eta}, \tag{32}$$

with

$$\eta = \frac{8}{3N\pi^2}. \tag{33}$$

An expansion around the origin of the analytic solution Eq. (27) gives as leading contribution

$$A(p) = 1/\left(1 - \frac{8}{3N\pi^2} \ln\left(p/\alpha\right)\right). \tag{34}$$

So although we do not find the anomalous behavior Eq. (32) explicitly, our result is in agreement with it to leading order in $1/N$. Moreover, our solution vanishes at $p \downarrow 0$, just like the suggested solution Eq. (32), and does not have the unphysical behavior of the perturbative result Eq. (31), which diverges at small momenta.

The results with the Ansatz 2 confirm this anomalous behavior of the wavefunction renormalization very well. In Fig. 3, we have also plotted the behavior Eq. (32), together with our numerical results using this Ansatz. This shows that our numerical results are in good agreement with the expectation of an anomalous dimension for the wavefunction renormalization, at least in the infrared region. In the ultraviolet region, Eq. (32) is not expected to be valid.

IV. DYNAMICAL MASS GENERATION

One of the interesting features of QED3 is that a fermion mass can be generated dynamically, breaking chiral symmetry. Starting with massless bare fermions, they can acquire a dynamical mass through nonperturbative effects. The order parameter for this symmetry breaking is the chiral condensate $\langle\bar{\psi}\psi\rangle$, but it is more convenient to consider the infrared value of $B(p)$ as the order parameter.

Writing the full fermion propagator as

$$S^{-1}(p) = A(p)\,\not{p} + B(p), \tag{35}$$

a nonzero solution for $B(p)$ implies a nonzero condensate, and signals dynamical mass generation. The infrared value of the dynamical mass function defined by $m(p) = B(p)/A(p)$, $m(0) = B(0)/A(0)$ can also be used as order parameter. Note we are not calculating the physical mass, defined at the pole of the propagator; this physical mass is expected to be in the Minkowski region, at least for observable particles, whereas we are performing our calculations completely in Euclidean region. The question of the existence of such a physical mass in the time-like region is not addressed here [13].

A. Existence of a critical number of flavors

Based on bifurcation theory, we can show that, for determining the critical number (if there is a critical number) of fermion flavors, it is sufficient to keep the terms which are linear in the generated mass, assuming that there is a continuous phase transition. This means that we can use the symmetric solutions for the vacuum polarization and wavefunction renormalization in the equation for B. To avoid infrared problems, we replace the denominator $A^2(k)k^2 + B^2(k)$ by $A^2(k)k^2 + B^2(0)$, and thus the equation for B reduces to[1]

$$B(p) = 2\,e^2 \int \frac{\mathrm{d}^3k}{(2\pi)^3} \frac{B(k)}{A^2(k)k^2 + B^2(0)} \frac{f(A(p), A(k), A(q))}{q^2 + \Pi(q)}\,, \tag{36}$$

or in terms of the mass function

$$m(p) = 2\,e^2 \int \frac{\mathrm{d}^3k}{(2\pi)^3} \frac{m(k)}{k^2 + m^2(0)} \frac{f(A(p), A(k), A(q))}{A(p)A(k)(q^2 + \Pi(q))}\,, \tag{37}$$

with A and Π as found in the previous section.

Consider first the Ansätze 3 and 5. They lead to

$$m(p) = 2\,e^2 \int \frac{\mathrm{d}^3k}{(2\pi)^3} \frac{m(k)}{k^2 + m^2(0)} \frac{1}{A(q)q^2 + \alpha q}\,, \tag{38}$$

and

$$m(p) = 2\,e^2 \int \frac{\mathrm{d}^3k}{(2\pi)^3} \frac{m(k)}{k^2 + m^2(0)} \frac{1}{q^2 + \alpha q}\,, \tag{39}$$

respectively. We note that these equations are qualitatively similar: in the infrared region, the part coming from the vacuum polarization, αq, will dominate over the other part, $A(q)q^2$ or q^2 respectively, whereas in the ultraviolet region $A(q) \simeq 1$. Thus, both Ansätze lead to almost the same equation for the mass function. Note that Eq. (39) is exactly the same equation for the mass function as one would get by using a bare vertex and neglecting the wavefunction renormalization completely [2].

Using the fact that the essential region for dynamical mass generation is the infrared region $p \ll \alpha$, we can use the scale α as an ultraviolet cutoff. This reduces both Eq. (38) and Eq. (39) to exactly the same equation, namely

$$m(p) = \frac{8}{N\,\pi^2} \int_0^\alpha \frac{\mathrm{d}k}{\max(p,k)} \frac{k^2 m(k)}{k^2 + m^2(0)}\,. \tag{40}$$

It is well-known that this equation leads to a critical number of fermion flavors for dynamical mass generation. This is seen directly by reducing it to a second-order differential equation

[1] Alternatively we could neglect the mass function in the denominator and introduce an infrared cutoff, which is generally identified with the infrared value of the mass function.

$$p^2 m''(p) + 2pm'(p) + \frac{8}{N\pi^2}\frac{p^2 m(p)}{p^2 + m^2(0)} = 0\,, \tag{41}$$

with boundary conditions. Below the critical number of fermion flavors, $N_c = 32/\pi^2 \simeq 3.24$, the solution is given by a hypergeometric function

$$m(p) = m(0)\ {}_2F_1\left(a_+, a_-, \tfrac{1}{2}; \frac{p^2}{m^2(0)}\right)\,, \tag{42}$$

with

$$a_\pm = \frac{1}{4} \pm \frac{i}{4}\sqrt{N_c/N - 1}\,. \tag{43}$$

As N approaches the critical number of fermion flavors, the infrared value of the mass function $m(0)$ decreases rapidly according to

$$m(0) = \alpha \exp\left[\frac{-2\pi}{\sqrt{N_c/N - 1}} + 3\ln 2 + \tfrac{1}{2}\pi\right]\,. \tag{44}$$

Above the critical number of flavors, the trivial solution $m(p) = 0$ is the only solution.

The equation for the dynamical mass function using the other Ansätze cannot so easily be obtained. However, using a simple counting argument, we can already expect that there is a critical number of fermion flavors, independent of the precise form of our Ansatz. In the infrared region, which is essential for dynamical symmetry breaking, we can neglect q^2 with respect to the vacuum polarization in the denominator $q^2 + \Pi(q)$. Counting the powers of A, we see that this vacuum polarization is roughly proportional to f/A^2, so the dependence of the integration kernel in Eq. (37) on the wavefunction renormalization and the vertex Ansatz might cancel out. This is similar to what we have already seen in the previous section, namely that the behavior of the wavefunction renormalization is almost independent of the vertex Ansatz we use.

Therefore, although the behavior of the vacuum polarization might depend on the vertex Ansatz, we expect that in fact the fermion propagator is not very sensitive to the precise Ansatz, due to a cancellation in the (far) infrared region between the implicit dependence of $\Pi(q)$ on the function $f(A(p), A(k), A(q))$, and the explicit appearance of this function in the integration kernel of Eq. (37). On these grounds one might expect a critical number of fermion flavors, independent of our choice for the vertex.

Even if we relax our requirement that the Ansatz goes to the bare vertex in the ultraviolet region, we find a similar result: consider for example the (unphysical) vertex

$$2\,A(p)A(k)\gamma^\mu\,. \tag{45}$$

This would lead to the equation for the mass function like

$$m(p) = 2\,e^2 \int \frac{\mathrm{d}^3 k}{(2\pi)^3}\frac{m(k)}{k^2 + m^2(0)}\frac{2}{q^2 + 2\alpha q}\,, \tag{46}$$

which has an additional factor of two. However, in the infrared region, this factor of two cancels against the additional factor of two which comes from the vacuum polarization, leading to the same critical number as with Ansatz 5.

Note that it is crucial for such a cancellation to occur that we consider the vacuum polarization with full propagators; using bare propagators in the loop for the vacuum polarization, is an inconsistent approximation. Formally, using such bare fermions in the loop for the vacuum polarization is in agreement with the $1/N$ expansion, but as we have seen in the previous section, the wavefunction renormalization is not of the order $1 + \mathcal{O}(1/N)$ in the infrared region. Therefore we should use the full propagators when calculating the vacuum polarization. Even when using bifurcation theory to calculate the critical number of fermion flavors, one should use the full propagators in the vacuum polarization, or to be more precise, the massless full propagators.

B. Numerical results

We can solve the coupled equations numerically for the mass function m (or for B), the wavefunction renormalization A, and the vacuum polarization Π in the broken phase. Starting with a trial function for B and the leading order contribution for the wavefunction, $A(p) = 1$, we can evaluate the vacuum polarization and solve the coupled equations for A and B. Next, we calculate the vacuum polarization, using these numerical solutions, and iterate this procedure until all three functions converge to a stable solution.

For the quenched approximation, $N = 0$, all five Ansätze lead to the same solution for B, since the vacuum polarization is zero in this case, and the wavefunction renormalization equal to one. This mass function is almost constant in the infrared region, and decreases rapidly, as $1/p^2$, at large momenta, for $p > e^2$. It agrees very well with earlier numerical studies of this approximation [4].

The typical behavior of the functions A, B, and Π is shown in Fig. 4 for several values of N. We note that the wavefunction renormalization decreases for small momenta, but does not vanish for $p \downarrow 0$: its value at the origin is nonzero, in contrast to the behavior in the symmetric phase. Also the behavior of the vacuum polarization is different: in the broken phase, the vacuum polarization behaves like p^2 in the (far) infrared region, so $\Pi(p)/p^2$ is finite at $p \downarrow 0$, whereas in the symmetric phase, $\Pi(p)/p^2$ blows up at the origin. The infrared behavior of the vacuum polarization is governed by the generated mass function: the smaller this mass function, the larger $\Pi(p)/p^2$. Finally the mass function, or rather B, is almost constant at small momenta, and decreases rapidly for large momenta. However, in the unquenched approximation, and especially close to the critical number of fermion flavors, we see *two* relevant mass scales [20]: $B(p)$ starts to decrease at the scale of the generated mass, but only beyond the energy scale α, it decreases like $1/p^2$. This phenomenon might be relevant for hierarchy problems in unified theories.

To determine the critical number of fermion flavors, we consider N as a continuous parameter in the DS equations. In Fig. 5, we show the infrared values of the wavefunction renormalization, of the scalar function B, and of the vacuum polarization, or rather of $\Pi(p)/p^2$, as functions of N. For increasing N, we note that $B(0)$ decreases, and that the infrared value of $\Pi(p)/p^2$ increases rapidly. Both functions indicate a critical value of the number of fermion flavors for dynamical mass generation, at which B vanishes, and where the limit $p \downarrow 0$ of $\Pi(p)/p^2$ diverges. Also the wavefunction renormalization at the origin decreases quite rapidly close to this critical number of flavors.

The dependence of $m(0)$ as function of N at fixed α is shown in Fig. 6. For comparison, we also included the analytical result Eq. (44). We see very clearly that the generated infrared mass also decreases very rapidly for increasing N, and the figure indicates a critical number of fermion flavors of about 3.3, more or less independent of the vertex Ansatz. The Ansätze 3, 4, and 5 give exactly the same critical behavior, and also Ansatz 2 leads to almost the same results. Only a bare vertex, Ansatz 1, indicates a slightly higher value for the critical number of flavors, but the general behavior is the same for all five Ansätze.

V. CONCLUSION

We have solved the *coupled* DS equations for the fermion propagator and the vacuum polarization, both in the chirally symmetric and in the broken phase, using a certain class of vertex functions. With this type of vertex, the behavior of the fermion propagator is almost independent of the exact form of the full vertex. We find a critical number for chiral symmetry breaking, $N_c = 3.3$, below which there is dynamical mass generation; above this critical number, only the chirally symmetric solution exists.

In the chirally symmetric phase, the wavefunction renormalization is approximately equal to one in the ultraviolet region, but in the infrared region, $A(p)$ vanishes, indicating an anomalous dimension. This non-uniform behavior of the wavefunction renormalization lies at the origin of a controversy about the existence of a critical number of fermion flavors. Also in the broken phase, $A(p)$ is not of the order one, as one might expect naively, but considerably smaller: as the number of fermion flavors approaches the critical number, $A(0)$ tends to go to zero. These results will also be relevant for studies of this model at finite temperature [27].

Our main result, a finite critical number of fermion flavors for dynamical mass generation, confirms the assertions obtained earlier by Appelquist *et al.* [2]. Their analysis was based upon a bare vertex and neglect of the wavefunction renormalization. There have been several claims that including the effects of the wavefunction renormalization leads to a different result, namely dynamical mass generation for all numbers of fermion flavors [6,7]. These and other studies, such as [8,9], show a crucial dependence on the behavior of the full vertex; in general a bare vertex or a vertex linear in the wavefunction renormalization would lead to chiral symmetry breaking for all N, whereas a vertex quadratic in A leads to a critical number of fermion flavors. However, all these studies include the wavefunction renormalization and an Ansatz for the full vertex in the fermion DS equation, but not in the vacuum polarization.

We would like to stress that in order to solve the DS equation for the fermion propagator self-consistently, we have to treat the fermion propagator nonperturbatively *both* in the fermion DS equation *and* in the equation for the vacuum polarization, at least if we are using the unquenched approximation. Also, one must use the same approximation for the full vertex in both the fermion and photon DS equation. It turns out that the effects of the wavefunction renormalization through the vacuum polarization change drastically the naive results obtained in [6–9]. In contrast to these earlier results, our results are almost independent of the vertex Ansatz.

For studying the chiral phase transition, one can use bifurcation theory and therefore neglect the dynamical mass function in the wavefunction renormalization. However, one

should keep in mind that bifurcation theory does not imply that one can use bare propagators in the vacuum polarization: one should use the chirally-symmetric full propagators. Of course, if the wavefunction renormalization is equal to one (as one often assumes in this kind of calculations), one can use the bare propagators to calculate the vacuum polarization.

We have made only one approximation in our calculation: replacing the full vertex by our Ansatz, Eq. (15). Of course, one could question this approximation, but our result is almost independent of the precise form of the function f. Furthermore, it has been shown that a next-to-leading order calculation in the context of the $1/N$ expansion also leads to a finite critical number of fermion flavors [3]. Our result is also in good agreement with lattice calculations [5].

ACKNOWLEDGEMENTS

I would like to thank Yoonbai Kim, Conrad Burden, K. Yamawaki, and Y. Hoshino for stimulating discussions and comments. This work has been financially supported by the Japanese Society for the Promotion of Science (JSPS fellowship No. 94146) and by a Grand-in-Aid for Scientific Research from the Japanese Ministry of Education, Science, and Culture (No. 90094146).

FIGURES

FIG. 1. The the numerical and analytical solutions for the wavefunction renormalization in the massless phase for $N = 6$, using the Ansätze 3 and 5.

FIG. 2. The numerical solutions in the massless phase for $N = 6$, using the Ansätze 1-5: (a) the wavefunction renormalization, (b) the vacuum polarization, and (c) the deviation of the vacuum polarization from the perturbative behavior.

FIG. 3. The wavefunction renormalization in the massless phase for $N = 2$, 4, 6, and 10, using Ansatz 2, together with the behavior based on the existence of an anomalous dimension.

FIG. 4. The functions $A(p)$, $B(p)$, and $\Pi(p)/p^2$ in the chirally broken phase for N = 0, 2, and 3, using Ansatz 2.

FIG. 5. The infrared values of the functions $A(0)$, $B(0)$, and $\lim_{p\to 0} \Pi(p)/p^2$ as functions of N at fixed e^2

FIG. 6. The infrared values of the mass function $m(0)$ as function of N at fixed α.

REFERENCES

* e-mail: maris@eken.phys.nagoya-u.ac.jp

[1] R.D. Pisarski, Phys. Rev. D **29**, 2423 (1984).
[2] T. Appelquist, M. Bowick, D. Karabali, and L.C.R. Wijewardhana, Phys. Rev. D **33**, 3704 (1986); T. Appelquist, D. Nash, and L.C.R. Wijewardhana, Phys. Rev. Lett. **60**, 2575 (1988).
[3] D. Nash, Phys. Rev. Lett. **62**, 3024 (1989).
[4] Y. Hoshino and T. Matsuyama, Phys. Lett. B **222**, 493 (1989).
[5] E. Dagotto, J.B. Kogut, and A. Kocić, Phys. Rev. Lett. **62**, 1083 (1989); E. Dagotto, A. Kocić, and J.B. Kogut, Nucl. Phys. B **334**, 279 (1990).
[6] M.R. Pennington and S.P. Webb, *Hierarchy of scales in three dimensional QED*, BNL-40886, January 1988 (unpublished); D. Atkinson, P.W. Johnson and M.R. Pennington, *Dynamical mass generation in three-dimensional QED*, BNL-41615, August 1988 (unpublished).
[7] M.R. Pennington and D. Walsh, Phys. Lett. B **253**, 246 (1991); D.C. Curtis, M.R. Pennington, and D. Walsh, Phys. Lett. B **295**, 313 (1992).
[8] D. Atkinson, P.W. Johnson, and P. Maris, Phys. Rev. D **42**, 602 (1990).
[9] K.-I. Kondo and H. Nakatani, Progr. Theor. Phys. **87**, 193 (1992).
[10] C.J. Burden and C.D. Robert, Phys. Rev. D **44**, 540 (1991).
[11] C.J. Burden, J. Praschifka, and C.D. Roberts, Phys. Rev. D **46**, 2695 (1992).
[12] G. Grignani, G. Semenoff, and P. Sodano, DFUPG-100-95, hep-th/9504105.
[13] P. Maris, hep-ph/9508323, Phys. Rev. D **52**, 6087 (1995).
[14] N. Dorey and N.E. Mavromatos, Nucl. Phys. B **386**, 614 (1992); I.J.R. Aitchison and N.E. Mavromatos, OUTP-95-32p, hep-th/9510058.
[15] E. Abdalla and F.M. de Carvalho Filho, MIT-CTP-2488, IC/95/350, hep-th/9511132.
[16] T. Appelquist, M.J. Bowick, D. Karabali, and L.C.R. Wijewardhana, Phys. Rev. D **33**, 3774 (1986).
[17] P.I. Fomin, V.P. Gusynin, V.A. Miransky and Yu.A. Sitenko, Nuovo Cimento **6**, 1 (1983); V.A. Miransky, Phys. Lett. B **146**, 401 (1985); Nuovo Cimento **90A**, 149 (1985).
[18] E.H. Simmons, Phys. Rev. D **42**, 2933 (1990).
[19] K.-I. Kondo and P. Maris, hep-ph/9408210, Phys. Rev. Lett. **74**, 18 (1995); hep-ph/9501280, Phys. Rev. D **52**, 1212 (1995).
[20] V.P. Gusynin, A.H. Hams, and M. Reenders, hep-ph/9509380, Phys. Rev. D **53**, 2227 (1996).
[21] K.-I. Kondo, hep-ph/9509345, Int. J. Mod. Phys. A **11**, 777 (1996).
[22] R.D. Pisarski, Phys. Rev. D **44**, 1866 (1991); G.W. Semenoff, P. Suranyi, and L.C.R. Wijewardhana, hep-ph/9502272.
[23] Seyong Kim and Yoonbai Kim, *Lattice Gauge Theory of Three-dimensional Thirring Model*, SNUTP-96-010.
[24] J.S. Ball and T.W. Chiu, Phys. Rev D **22**, 2542 (1980).
[25] A. Kizilersü, M. Reenders, and M.R. Pennington, hep-ph/9503238, Phys. Rev. D **52**, 1242 (1995).
[26] T.W. Appelquist and U. Heinz, Phys. Rev. D **24**, 2169 (1981).
[27] I.J.R. Aitchison and M. Klein-Kreisler, hep-ph/9402213, Phys. Rev. D **50**, 1068 (1994).

Figure 1

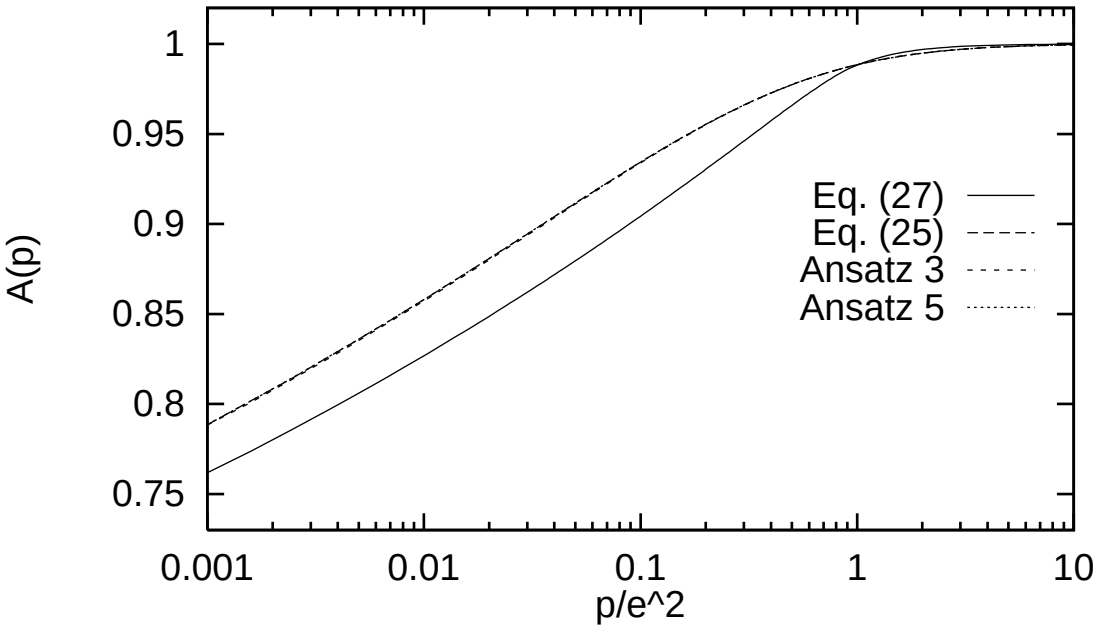
A(p)
1
0.95
0.9
0.85
0.8
0.75
0.001
0.01
0.1
1
10
p/e^2
Eq. (27)
Eq. (25)
Ansatz 3
Ansatz 5

Figure 2

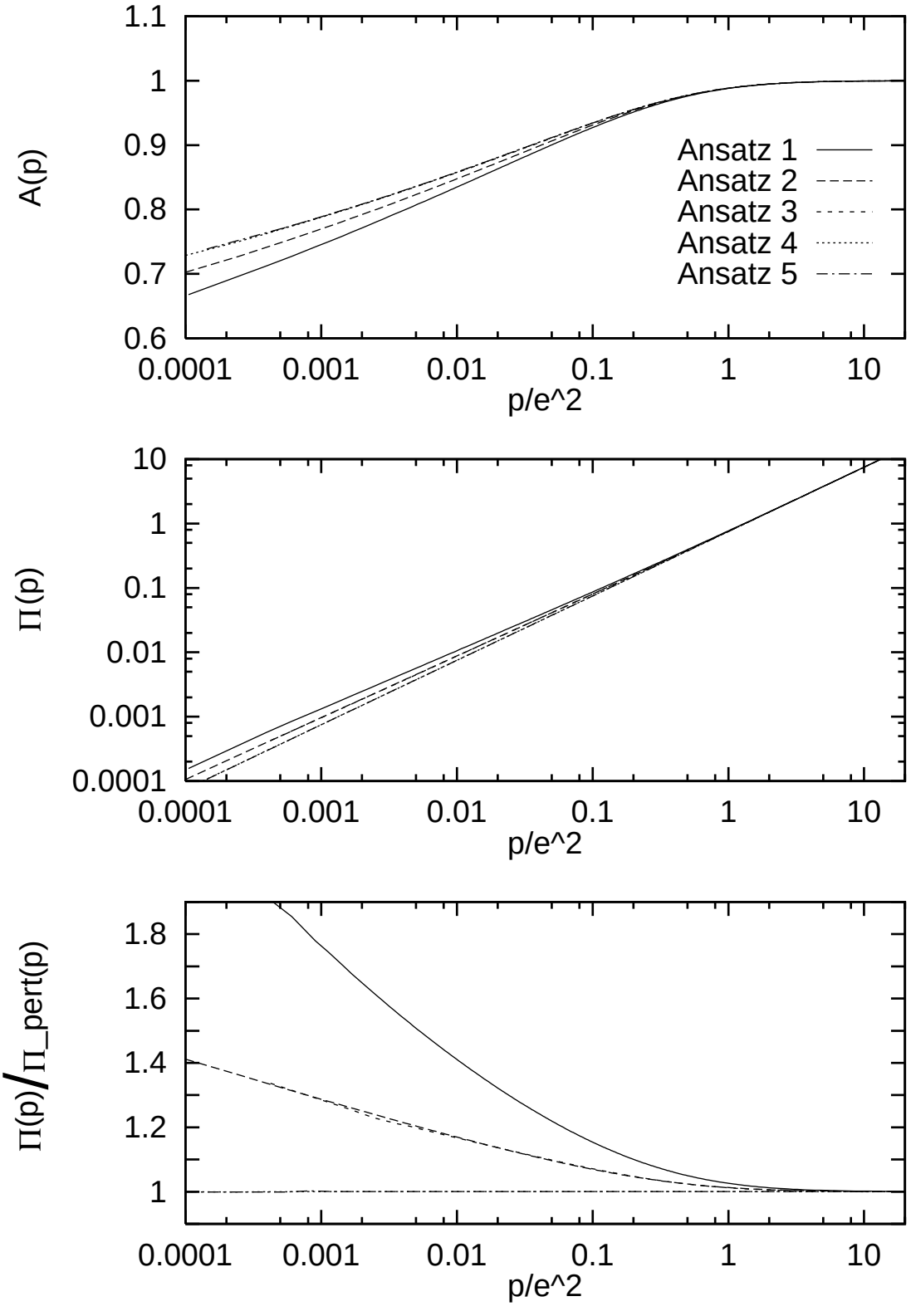
A(p)
1.1
1
0.9
0.8
0.7
0.6
0.0001
0.001
0.01
0.1
1
10
p/e^2
Ansatz 1
Ansatz 2
Ansatz 3
Ansatz 4
Ansatz 5
Π(p)
10
1
0.1
0.01
0.001
0.0001
0.0001
0.001
0.01
0.1
1
10
p/e^2
Π(p)/Π_pert(p)
1.8
1.6
1.4
1.2
1
0.0001
0.001
0.01
0.1
1
10
p/e^2

Figure 3

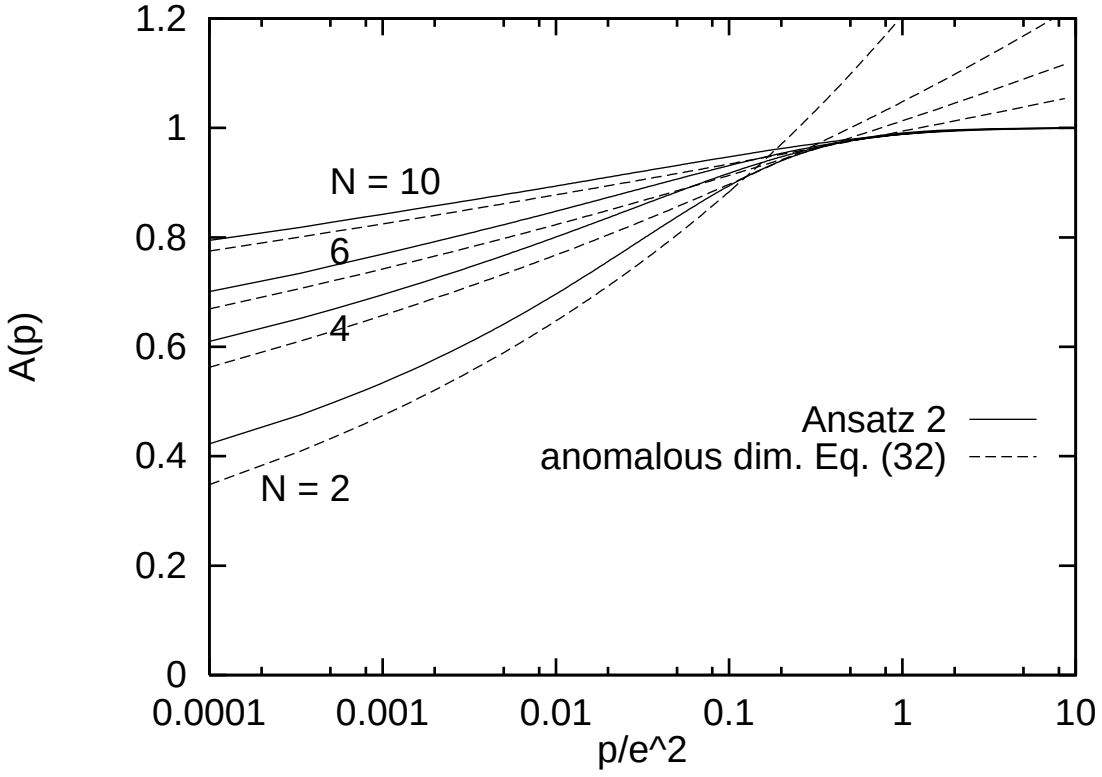
1.2
1
0.8
0.6
0.4
0.2
0
A(p)
N = 10
6
4
N = 2
Ansatz 2
anomalous dim. Eq. (32)
0.0001
0.001
0.01
0.1
1
10
p/e^2

Figure 4

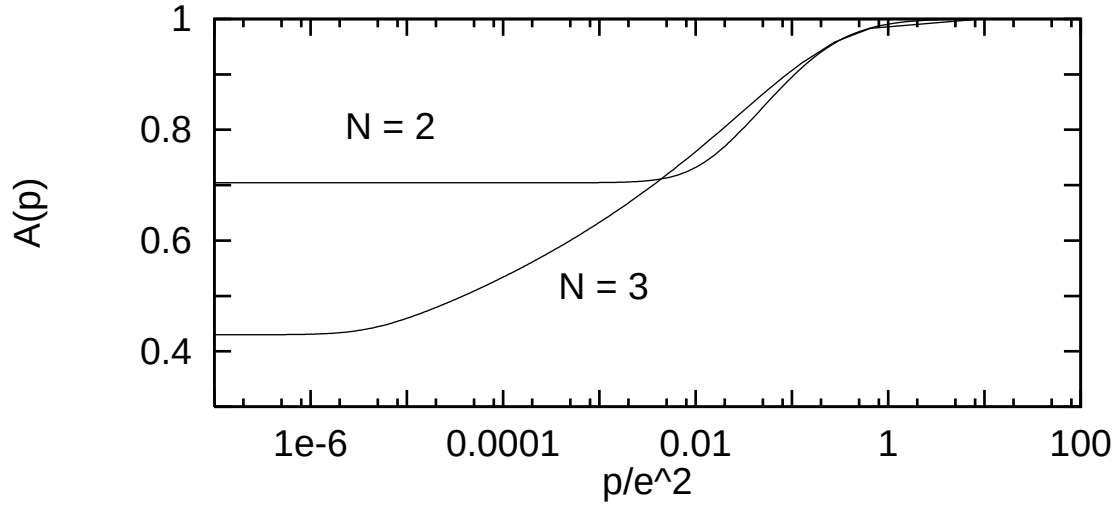
A(p)
1
0.8
0.6
0.4
N = 2
N = 3
1e-6
0.0001
0.01
1
100
p/e^2

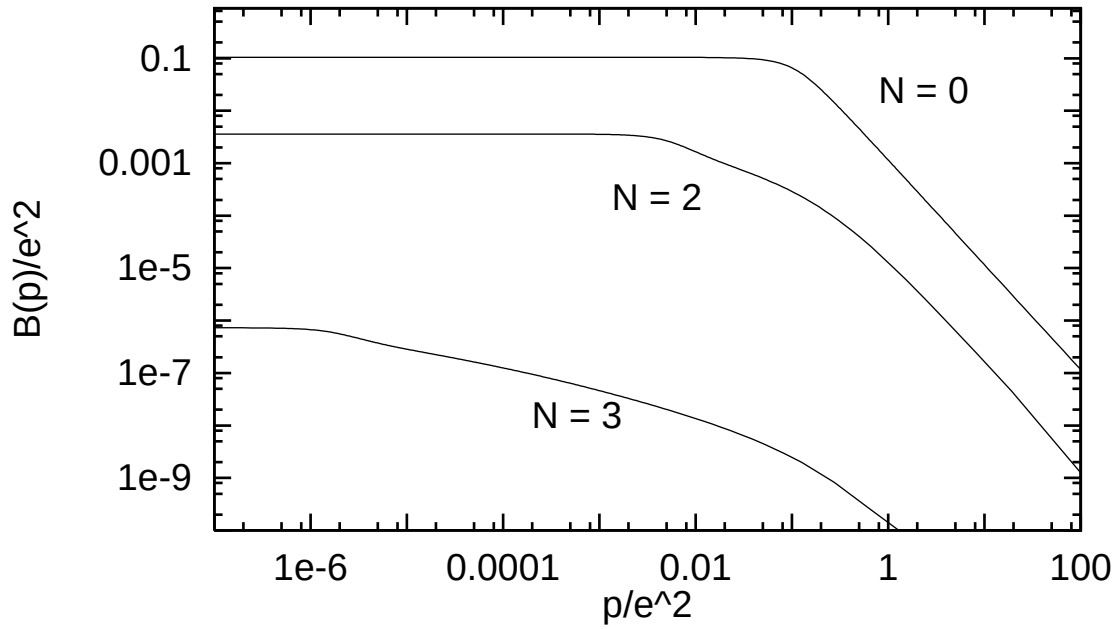
B(p)/e^2
0.1
0.001
1e-5
1e-7
1e-9
N = 0
N = 2
N = 3
1e-6
0.0001
0.01
1
100
p/e^2

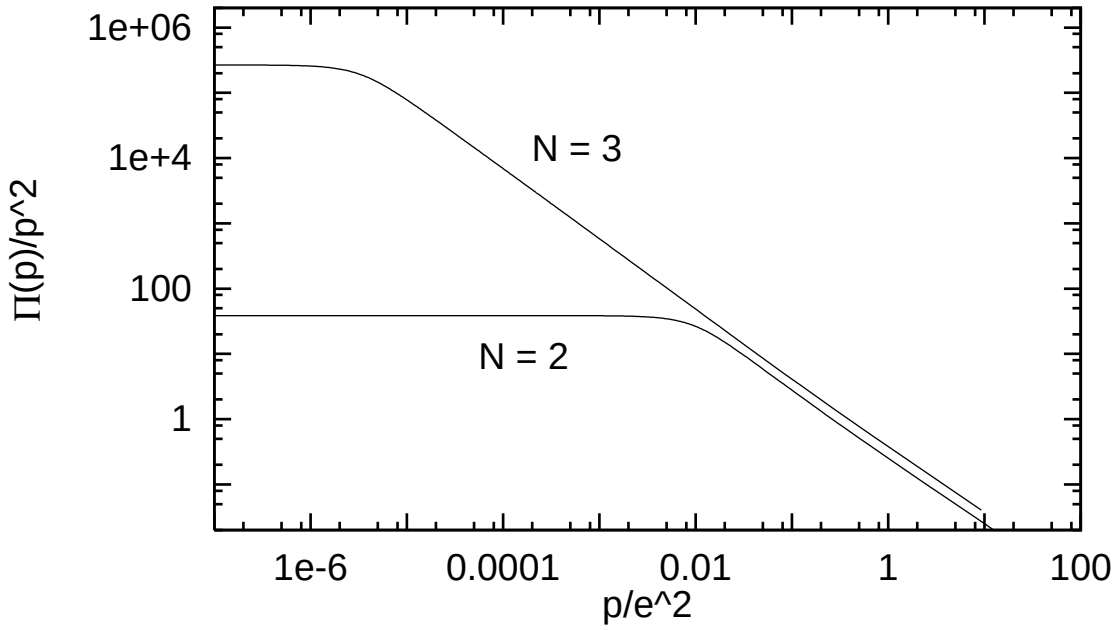
Π(p)/p^2
1e+06
1e+4
100
1
N = 3
N = 2
1e-6
0.0001
0.01
1
100
p/e^2

Figure 5

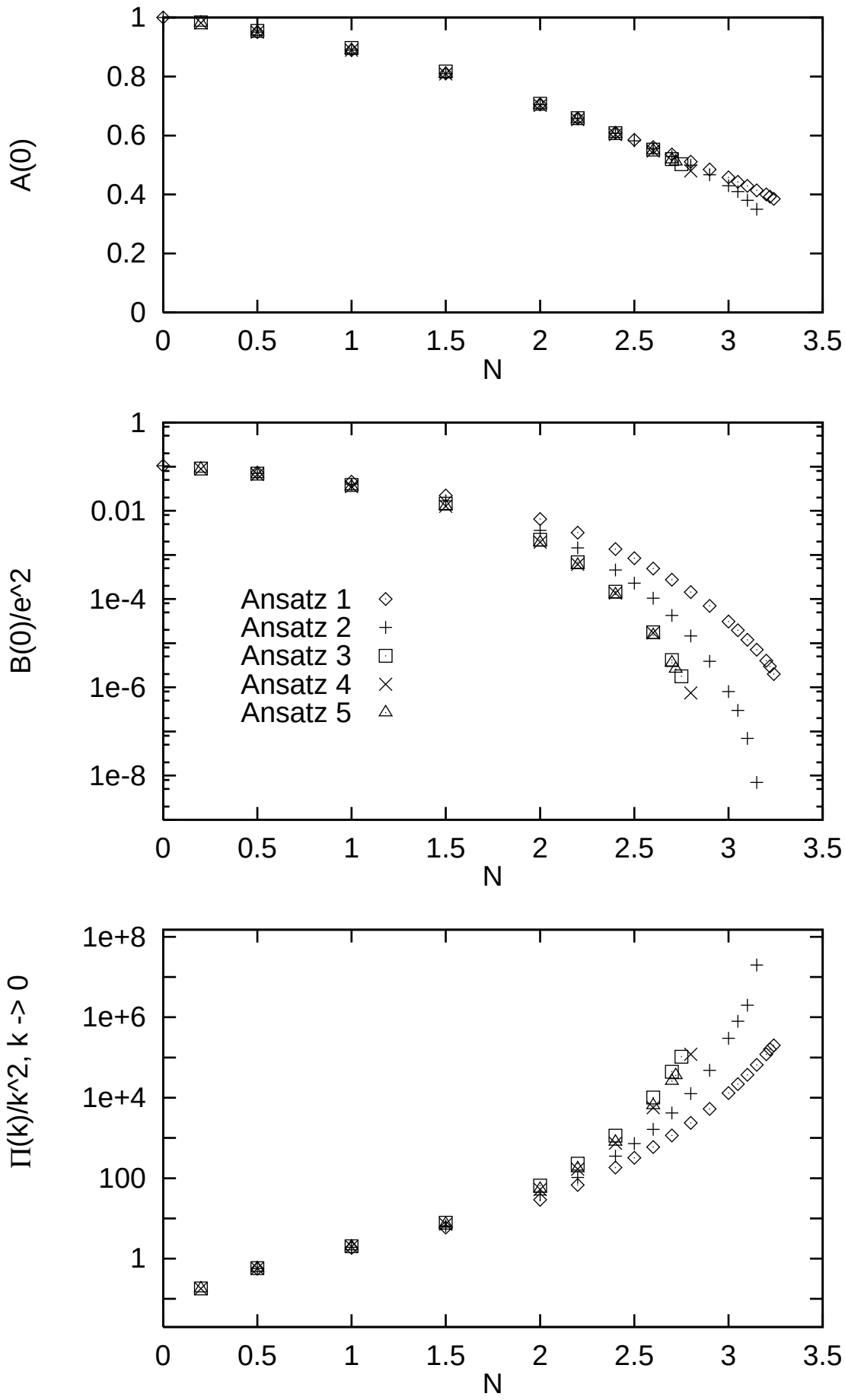
A(0)
1
0.8
0.6
0.4
0.2
0
0
0.5
1
1.5
2
2.5
3
3.5
N
B(0)/e^2
1
0.01
1e-4
1e-6
1e-8
Ansatz 1
Ansatz 2
Ansatz 3
Ansatz 4
Ansatz 5
Π(k)/k^2, k -> 0
1e+8
1e+6
1e+4
100
1

Figure 6

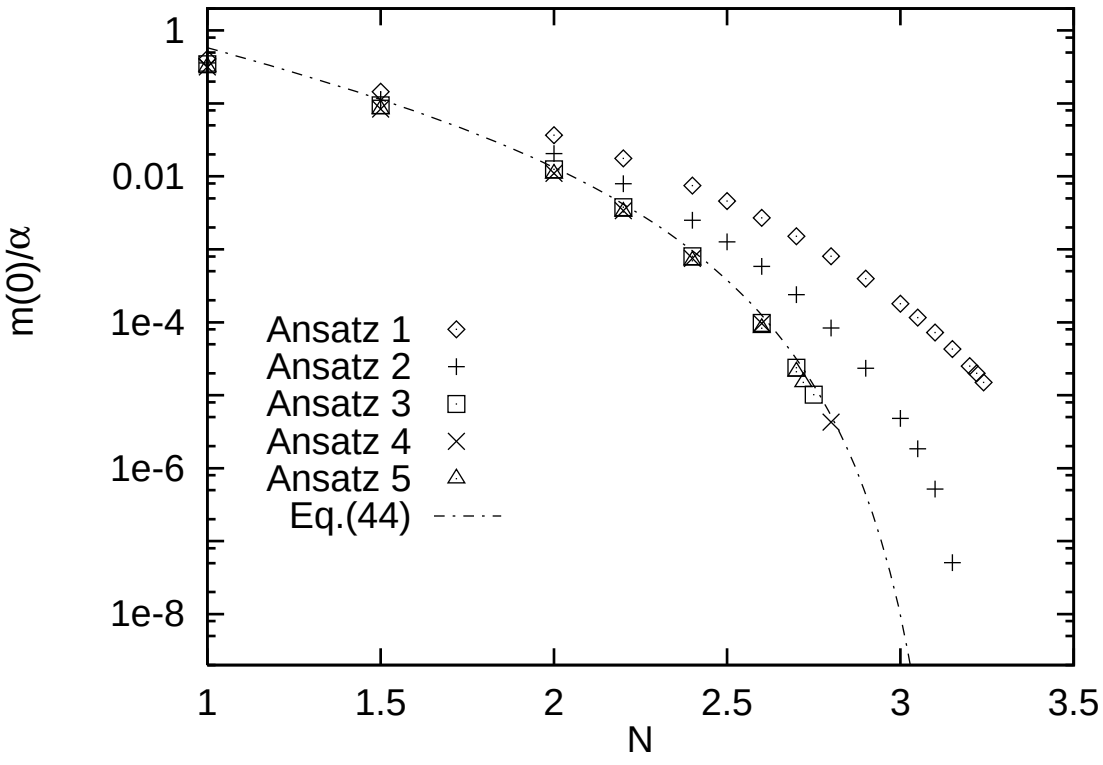
m(0)/α
1
0.01
1e-4
1e-6
1e-8
1
1.5
2
2.5
3
3.5
N
Ansatz 1
Ansatz 2
Ansatz 3
Ansatz 4
Ansatz 5
Eq.(44)